A New Topological Class of Interlocked and Interwoven Nanocarbons *via* Dynamic C-C Bond Formation

Harrison M. Bergman,[1] Angela Fan,[1] Christopher G. Jones,[2,3] August J. Rothenberger,[1] Kunal K. Jha,[3] Rex C. Handford,[1] Hosea M. Nelson,[2,3] Yi Liu,[4] T. Don Tilley[1]

[1]Department of Chemistry, University of California, Berkeley, Berkeley, California 94720, United States

[2]Department of Chemistry and Biochemistry, University of California, Los Angeles, Los Angeles, California 90095, United States

[3]Division of Chemistry and Chemical Engineering, California Institute of Technology, Pasadena, California 91125, United States

[4]Molecular Foundry, Lawrence Berkeley National Laboratory, Berkeley, California 94720, United States

Abstract

Topologically complex molecules are poised to play a crucial role in the future of materials science, providing control over entanglement at the smallest possible scale. Discovery of new topological constructs and robust strategies for their synthesis are central to expanding the field. Here a new topological class of molecules, named perplexanes, are identified that contain an unusual combination of interlocking and interweaving that defies traditional topological descriptors. Two nanocarbon perplexanes are rationally synthesized in high yield using reversible zirconocene coupling of alkynes. This dynamic C-C bond formation facilitates entanglement under thermodynamic control, enabling the use of simple precursors without the need for strong templating or preassembly. This provides a new toolkit for assembling topologically complex nanocarbons that should be generalizable to a wide range of other topologies.

One Sentence Summary

A new synthetic approach enables the synthesis of carbon nanostructures with unprecedented topological complexity.

Introduction

Topological complexity is ubiquitous on the macroscale, where interlocking, braiding, and interweaving motifs underpin valuable technologies like textiles and building materials. Increasingly, topology is also being recognized as a critical design element on the nanoscale, since modes of entanglement in polymers and other extended systems have drastic effects on physical properties.[1–5] In comparison, entanglement as a molecular property is still in its infancy. For molecular entities, a range of relatively simple topologies have been identified[6,7] – largely types of knots, catenanes, and rotaxanes. These molecular systems are expected to exhibit unusual properties and have already found applications in anion-binding and catalysis,[8] photophysics,[9,10] membrane transport,[11] and supramolecular chemistry.[12] To further interrogate the chemical implications of molecular topology, it is necessary to develop convenient synthetic pathways that expand the breadth of accessible topologies and chemical functionalities in these systems.

Many of the entangled molecules realized to date are mathematically described as knots or links: one or multiple rings that are interwoven and/or interlocked, defined by their number of crossing points. Increasing topological complexity has therefore focused largely on increasing the

number of structural "crossings", up to the current maximum of twelve.[13–16] This approach, however, generally requires increasingly complex precursors and severely challenges the current limits of synthetic chemistry. A different approach to increase topological complexity is with the introduction of branching points, moving from monocyclic to polycyclic constituents. While the latter can be assembled from relatively simple building blocks, they are not easily described by mathematical nomenclature, and the large variety of potential topologies greatly complicates the rational design of synthetic routes to specific structures. Ravels have been identified as one general class of branched entangled structures,[17,18] and Fujita and coworkers have developed another class, broadly described as “entangled polyhedra”.[19–21] This represents an exciting new path forward, but chemical diversity in these systems remains low, relying on metal nodes that limit the electronic and mechanical properties, and stability, of these materials. Further development of this approach requires conceptually new frameworks for organizing the resulting structures, and new design strategies to facilitate more chemical diversity.

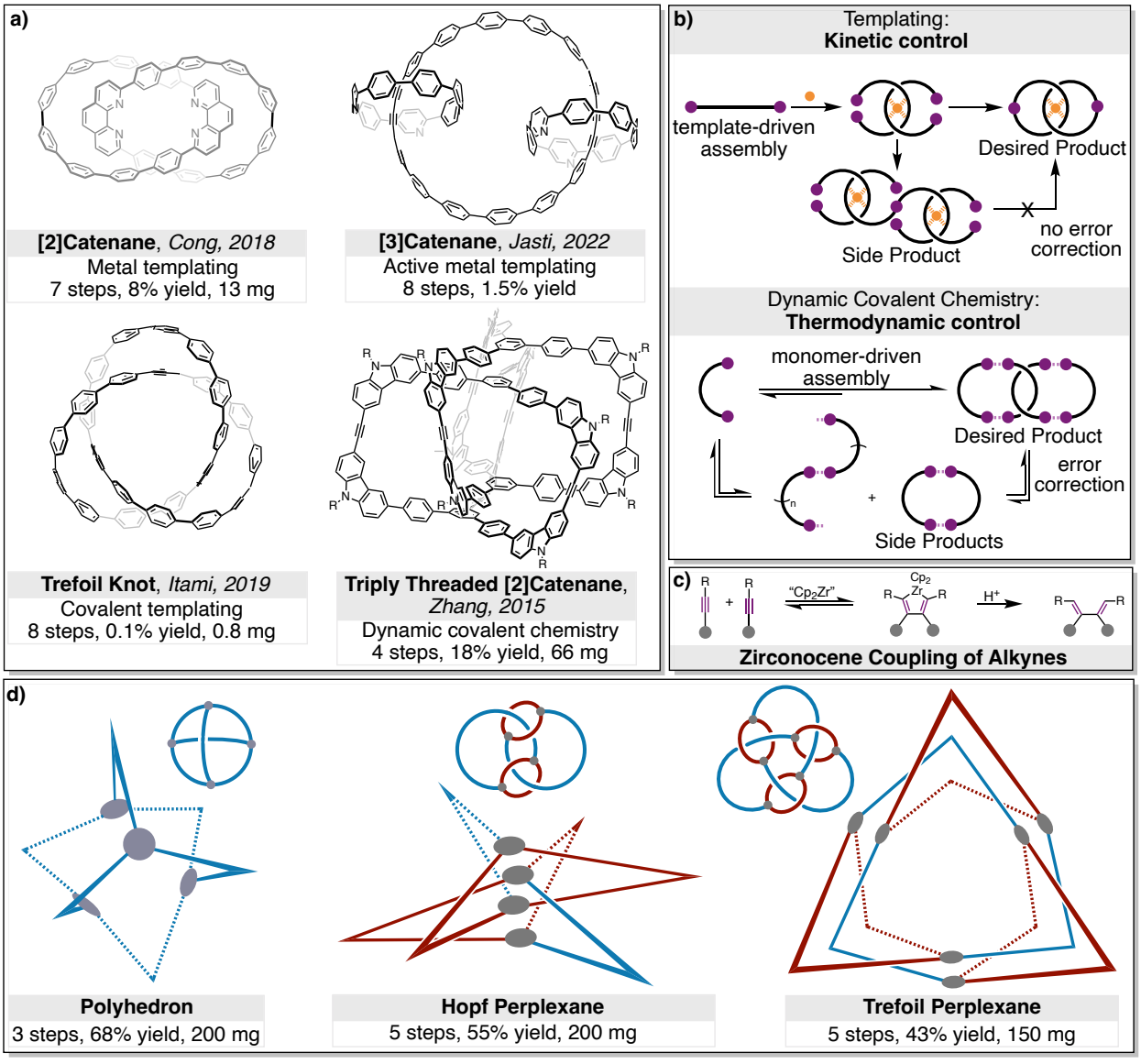

Figure 1. Summary of prior work on the synthesis of topologically complex nanocarbons and the advances introduced in this report. (a) representative examples of reported topologies and synthetic strategies; (b) schematic highlighting the differences between kinetic and thermodynamic synthetic control; (c) the reversible C-C bond forming reaction type used in this work; and (d) the three topologies rationally designed using this approach.

Carbon nanomaterials, such as graphene, carbon nanotubes, and fullerenes, display a wide range of desirable behaviors due to their carbon-rich, unsaturated frameworks. This motivates the incorporation of these structural motifs into topologically complex structures to greatly expand the breadth of applications for interlocked and interwoven molecules. However, to date only a few simple topologies of the latter type have been realized (Figure 1a), all with the assistance of covalent or metal coordination-based templating. These include Bäuerle's oligothiophene [2]catenanes obtained *via* copper-phenanthroline assemblies (9 steps, 5% yield),[22,23] Cong's [2]catenane nanohoops prepared using copper coordination (7 steps, 8% yield, 13 mg)[24] and diazo covalent templates (8 steps, 1.5% yield, 14 mg),[25] Itami's all-phenylene [2]catenanes and trefoil knot *via* a cleavable spirosilane (7-8 steps, 0.1-2% yield, 0.8-2 mg)[26,27] and Jasti's nanohoop rotaxanes and catenanes, recently obtained with use of active metal templating (8 steps, 1.5% yield).[28]

As illustrated by these pioneering examples, the creation of C_{sp2}-hybridized, entangled structures is still a formidable synthetic challenge as it requires a highly specific order and spatial arrangement of C-C bond formations to selectively construct the desired architecture. Most synthetic methods for generating C_{sp2}- C_{sp2} bonds involve irreversible coupling reactions that do not provide preferred orientations or any means for error correction. This necessitates the use of strong directional templating to kinetically favor the entangled product, but such templates generally require several synthetic steps and highly specific functional groups. The rigidity and planarity of the aromatic building blocks present additional synthetic constraints for forming entangled structures.

Dynamic covalent chemistry (DCvC) offers a potential solution to these synthetic challenges by providing a mechanism for error correction during molecular assembly.[29] A reversible bond-forming reaction allows the system to funnel to the most thermodynamically favored structure without the need for strong templating or other preorganization. However, the application of DCvC to entangled nanocarbons has been limited by the lack of reversible C_{sp2}-C_{sp2} bond forming reactions. There is currently only one report of a topologically complex nanocarbon synthesized using dynamic covalent chemistry, Zhang's formation of a triply threaded [2]catenane based on alkyne metathesis.[30] The shorter synthesis and higher yield highlight the promise of this alternate approach, but the structure was not confirmed crystallographically and the method has not been generalized since the initial publication.

Progress in this area can be facilitated by simple, generalizable syntheses that combine interweaving (knotting) and interlocking motifs for development of new topological classes of molecules. Interestingly, we recognized that triply threaded catenanes such as Zhang's constitute the simplest case of one such class that has not yet been identified or generalized. This novel topological class can be generated by replacing each crossing point in a traditional link or knot with a threaded macrocycle, as illustrated in Figure 2. These structures are notable for containing an otherwise unexplored combination of topological features, namely rotaxane-like interlocking with knot-like interweaving. Due to the lack of a well-recognized term for such structures, we propose the name *perplexane*, derived from the Latin word "perplexus" which means "entangled". For an in-depth discussion of the underlying topology, see pages S14-S15 in the supporting information.

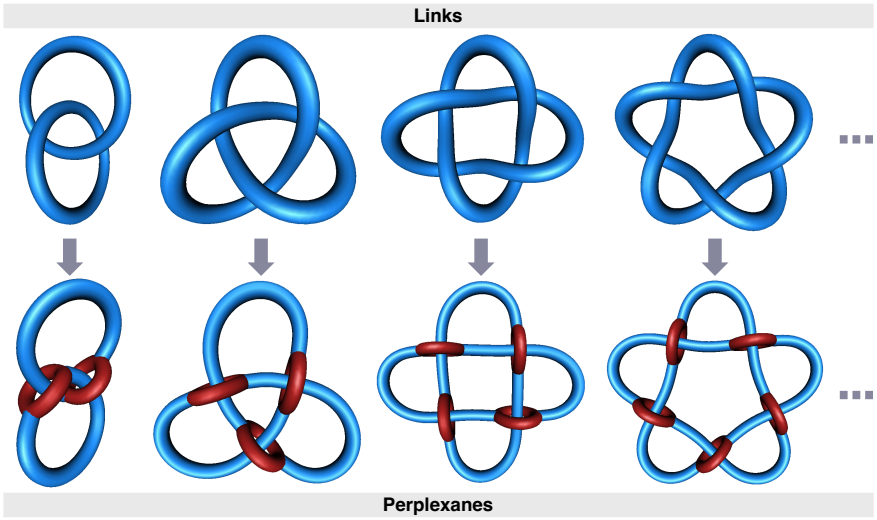

Figure 2. The derivation of perplexanes (bottom row) from four representative "parent" links via interconversion of crossing points to threaded loops (left to right): hopf link, trefoil knot, Solomon link, and pentafoil knot.

Here we introduce a general strategy to access nanocarbon perplexanes using a reversible alkyne coupling to form C_{sp2}-C_{sp2} bond linkages. This enables the high-yield formation of topologically complex structures in the absence of strong preorganization (Figure 1c). The size and topology of these structures can be rationally controlled by monomer design, as illustrated below by the synthesis of three topologically distinct cage structures: a polyhedron, a hopf perplexane, and the first trefoil perplexane (Figure 1d).

Results and Discussion

Monomers were designed using conceptually simple combinations of a structural core and associated "linkers". In this design, the core consists of a rigid, planar conjugated system that controls size and directs monomer assembly, while the linker provides the required flexibility for interdigitation. Conformational flexibility is achieved with the incorporation of a thiophene unit, which introduces a wide bite angle and can adopt a range of dihedral angles with respect to the core.

First, an alkynylated triphenyltriazine (TPT) monomer **1-mon**, containing no flexible linker (Figure 3), was investigated. It was anticipated that this monomer would form a simple polyhedron with no entanglement. Upon treatment with $Cp_2Zr(Me_3SiC{\equiv}CSiMe_3)(pyr)$ (a synthon for zirconocene, Cp_2Zr)[31,32] in THF, a complex mixture of products formed at 23 ˚C and persisted upon heating to 80 ˚C. However, after heating to 100 ˚C the mixture converged to a single major

species, **1-Zr**, in 81% yield on a 200 mg scale. Changing the reaction solvent to benzene caused the same product to precipitate from the reaction mixture as single crystals. X-ray crystallography of **1-Zr** determined the structure to be a tetrameric polyhedron (Figure 4a). The **1-Zr** cage was quantitatively demetalated by treatment with HCl in benzene, to provide the fully organic structure **1**. The retention of the polyhedral structure was confirmed by ^{1}H NMR spectroscopy and MALDI-MS analysis (Supporting information page S6). This cage topology mirrors the [4+6] cages synthesized by Fujita[33] and Cooper[34] via dynamic chemistry. However, while those approaches furnish structures with weak C-heteroatom or metal coordination bonds, **1** is connected by strong C-C bonds that display robust stability.

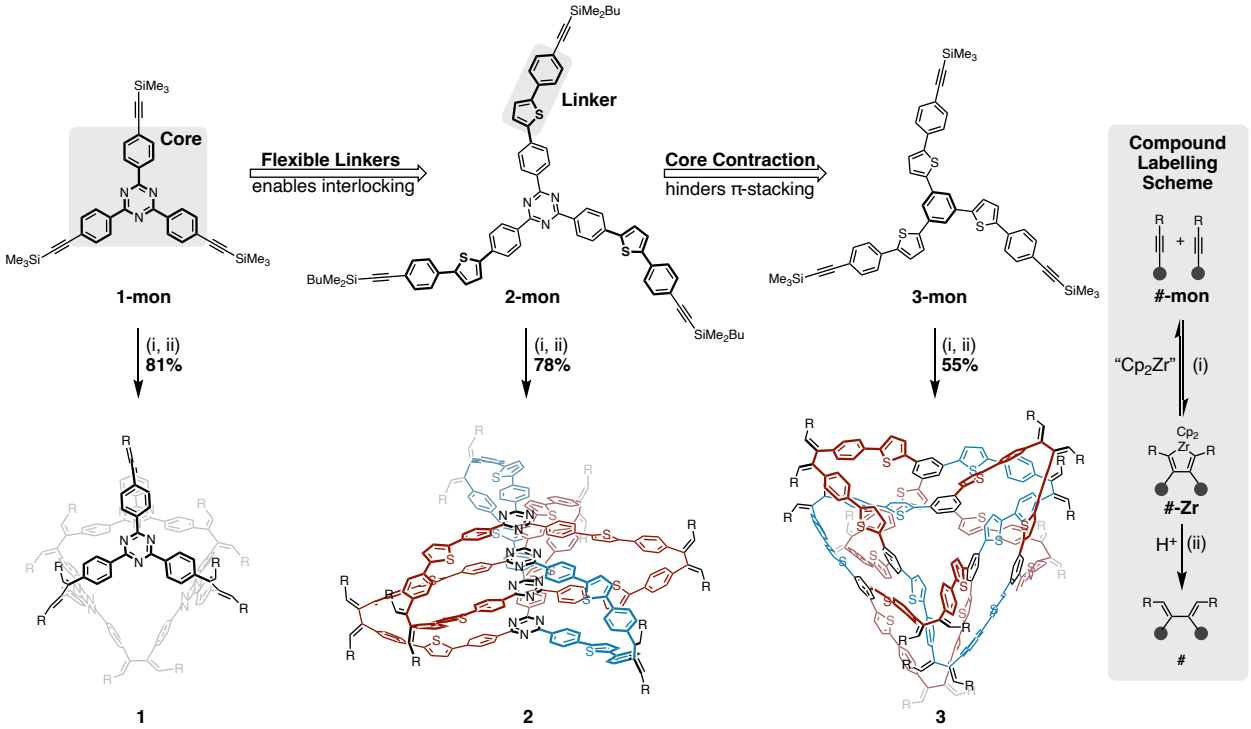

Figure 3. Synthesis of **1-3**. Reagents and conditions. (i) $Cp_2Zr(Me_3SiC{\equiv}CSiMe_3)$(pyr), benzene, 60 ˚C. (ii) HCl, THF, 23 ˚C.

Next, a Hopf perplexane was targeted as the simplest example of this new topological class. The TPT core is well suited for this due to its propensity for π-stacking into well-defined aggregates.[35,36] Monomer **2-mon** was generated by introducing the flexible thienylene-phenylene linker to the TPT core. Upon treatment with $Cp_2Zr(Me_3SiC{\equiv}CSiMe_3)$(pyr) in THF, a single major species, **2-Zr**, formed rapidly upon heating to 60 ˚C, and was isolated in 78% yield on a 200 mg scale. Product formation appears to be invariant to concentration, suggesting a significant enthalpic driving force.

Perplexane **2-Zr** was crystallized in a manner analogous to that for **1-Zr**, to form hexagonal crystals that are ~20 µm in diameter. Given the small size and distinct morphology of the crystals, **2-Zr** was subjected to microcrystal electron diffraction (microED) for initial characterization efforts. While the resulting electron diffraction data did indeed yield well-defined single-crystal diffraction, resolution beyond 3.0 Å was not obtainable; thus, a direct methods solution from such data could not be achieved. Despite its low resolution, electron diffraction data confirmed the single-crystalline nature of the material and thus, subsequent synchrotron experiments yielded sub-angstrom data sufficient for the successful structural resolution of **2-Zr**. Upon resolution, it exhibited a large unit cell volume of 44734 $Å^3$ and significant electron density associated with solvent in the intermolecular void spaces of the cell.

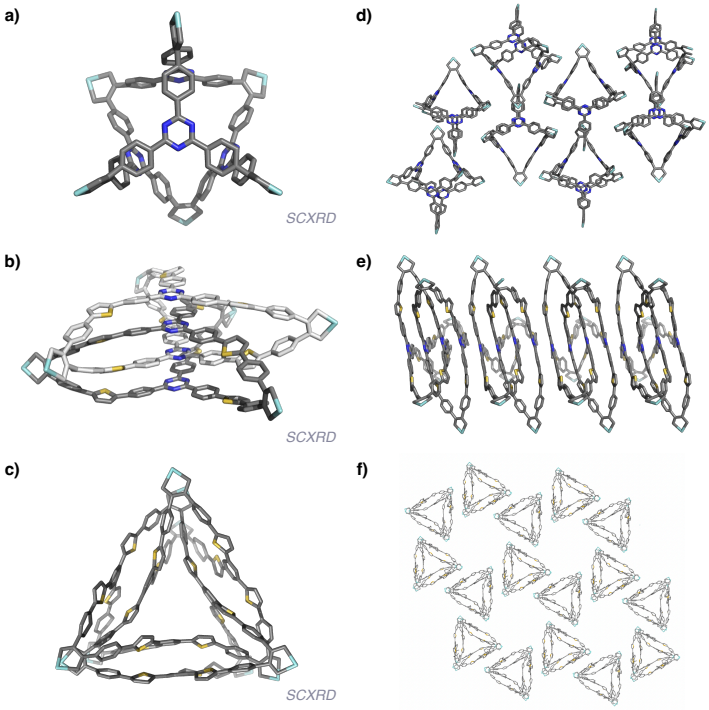

Figure 4. X-ray crystallographic structures of **1-Zr** (a, d), **2-Zr** (b, e), and **3-Zr** (c, f) with all sidechains, solvent, and hydrogens truncated for clarity. (a-c) individual cages; (d-f) solid-state packing.

The residual solvent was highly disordered and could not be modeled during refinement. Additionally, despite best efforts, several butyl groups on the $SiMe_2Bu$ moiety remained highly disordered, preventing their complete resolution. While these groups may not be fully resolved, the primary structure is well defined and successfully corroborates spectroscopic data to confirm the formation of **2-Zr**. As with **1**, metal-free **2** was generated *via* quantitative demetallation as confirmed by MALDI-MS analysis and ^{1}H NMR spectroscopy (Supporting Information page S7).

Analysis of the crystal structure of **2-Zr** highlights the role of both the core and linker in its assembly. Strong intramolecular π-stacking is observed between TPT cores, with an average distance of 3.3 Å, suggesting that catenane formation is largely driven by these core-core interactions. Compound **2-Zr** also forms ordered 1D columns in the solid state, driven by similarly strong intermolecular core-core π-stacking (Figure 4e). The linker accommodates this close packing of the cores by adopting a largely planar conformation, with an average thiophene-triazine dihedral angle of only ~21˚.

To quantify the strength of the monomer-monomer interactions in solution, the aggregation of a more soluble analog of **2-mon** with octyl instead of butyl chains, **2-mon-oct**, was studied by variable-concentration ^{1}H NMR spectroscopy. The concentration of **2-mon-oct** was varied over an order of magnitude between 0.8 and 46 mM in benzene-d_6 at 23 ˚C. The chemical shift of each aromatic peak was plotted as a function of concentration and fitted with good agreement to a monomer–dimer equilibrium model (Figure 5a). This model indicated K_a = 15 ± 2 M^{-1} and ΔG = -

1.6 ± 0.4 kcal/mol. Assuming no cooperative or anti-cooperative effects, this suggests that π-stacking provides an approximate 4.5 kcal/mol driving force for catenane assembly.

This efficient formation of π-stacked tetramers posed a design challenge for targeting higher order perplexane structures. However, decreasing the size of the monomer core was expected to diminish π-stacking and geometrically inhibit the formation of an analogous tightly interlocked catenane, while enabling thermodynamic pathways to other structures. To achieve this, the TPT core was replaced by a trisubstituted benzene ring with the synthesis of **3-mon**.

Unlike the coupling of **2-mon**, the reaction of **3-mon** with $Cp_2Zr(Me_3SiC{\equiv}CSiMe_3)(pyr)$ at 60 ˚C and 5.5 mM did not cleanly furnish a single product. The product formation is highly sensitive to concentration (by ^{1}H NMR spectroscopy), with higher concentrations favoring low-symmetry **3-Zr** (Figure 4c). At 56 mM, **3-Zr** was the sole well-defined product, and was isolated in 55% yield on a 150 mg scale. X-ray crystallographic analysis was accomplished in the same manner as for **2-Zr** and revealed the structure to be a highly entangled, fully continuous hexamer (Figure 4c). In contrast to those of **2-Zr**, crystals of **3-Zr** provided excellent quality data allowing atomic resolution of the structure in its entirety with minimal disorder, despite the large unit cell of 87813 Å^3 and the large number of solvent molecules within the crystal lattice. Compound **3** was generated from **3-Zr** under conditions identical to those used for **1** and **2**. Notably, while **3-mon** is insoluble in hexanes and only sparingly soluble in chlorinated solvents like DCM and chloroform, **3** is exceptionally soluble in hexanes (35 mg/mL) despite having a near-identical chemical composition and much higher molecular weight. This counterintuitive solubility highlights the unique dynamics of such densely intertwined structures.

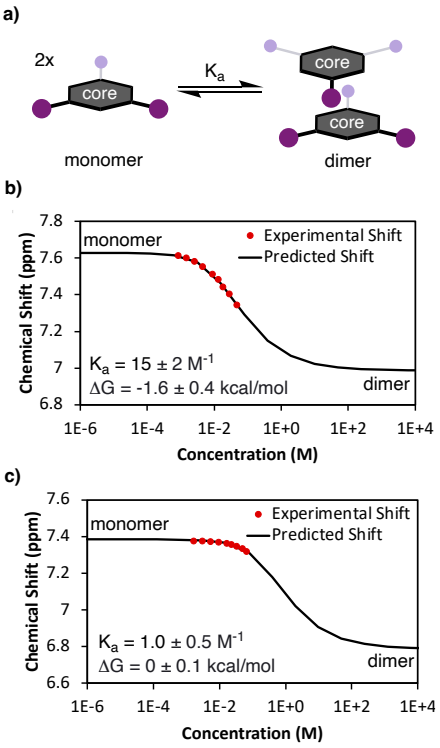

Figure 5. Fitting of variable concentration ^{1}H NMR data to the monomer-dimer equilibrium model depicted in (a) for (b) **2-mon-oct**, and (c) **3-mon-oct**.

In good agreement with expectations, there is no intramolecular π-stacking between monomers in the crystal structure, with an average core-core distance of 4.1 Å. This suggests that assembly is instead driven by weak dispersion interactions and a minimization of free volume. Similarly, the assembly of hexagonal arrays in the solid state appears to be driven only by weak intermolecular dispersion interactions (Figure 4f).

Variable concentration ^{1}H NMR measurements of a soluble analog of **3-mon**, **3-mon-oct**, dissolved in benzene-d_6, between 1.7 and 67 mM, corroborate the absence of strong attractive monomer interactions, with K_a = 1.0 ± 0.5 M^{-1} and ΔG = 0.0 ± 0.1 kcal/mol (Figure 5b). The formation of this highly complex hexameric structure in the absence of any templating or strong thermodynamic driving force highlights the utility of a dynamic approach to topological nanocarbon synthesis.

Conclusion

Topological complexity is now recognized to play a crucial role in determining the properties of materials across several length scales, from the molecular to nano- and microscale. Progress will depend on discovery of key design principles that correlate structures with properties, and development of synthetic methods that allow encoding of specific, molecular-scale elements of entanglement. The topological class introduced here, the *perplexanes*, is characterized by a high density and diversity of entanglements which may imbue them with dynamic and mechanical behaviors that are distinct from those of previously synthesized knots and catenanes. Synthetic access to this level of structural complexity is indeed quite challenging, and advances are expected to rely on new insights into the control of supramolecular preassembly of monomer units. The topological space encompassing higher perplexanes and wholly new structural types can be expanded with the application of dynamic covalent chemistry, especially with approaches that generate multiple, robust C-C bonds in a single synthetic step as demonstrated with the zirconocene-coupling strategy described here. Future efforts will then focus on studying the unique dynamics in these systems, both in solution and as building blocks for extended solids.

References

(1) Gotoh, H.; Liu, C.; Imran, A. B.; Hara, M.; Seki, T.; Mayumi, K.; Ito, K.; Takeoka, Y. Optically Transparent, High-Toughness Elastomer Using a Polyrotaxane Cross-Linker as a Molecular Pulley. *Sci. Adv.* **2018**, *4* (10), eaat7629. https://doi.org/10.1126/sciadv.aat7629.

(2) Jiang, Y.; Zhang, Z.; Wang, Y.-X.; Li, D.; Coen, C.-T.; Hwaun, E.; Chen, G.; Wu, H.-C.; Zhong, D.; Niu, S.; Wang, W.; Saberi, A.; Lai, J.-C.; Wu, Y.; Wang, Y.; Trotsyuk, A. A.; Loh, K. Y.; Shih, C.-C.; Xu, W.; Liang, K.; Zhang, K.; Bai, Y.; Gurusankar, G.; Hu, W.; Jia, W.; Cheng, Z.; Dauskardt, R. H.; Gurtner, G. C.; Tok, J. B.-H.; Deisseroth, K.; Soltesz, I.; Bao, Z. Topological Supramolecular Network Enabled High-Conductivity, Stretchable Organic Bioelectronics. *Science* **2022**, *375* (6587), 1411–1417. https://doi.org/10.1126/science.abj7564.

(3) Kim, J.; Zhang, G.; Shi, M.; Suo, Z. Fracture, Fatigue, and Friction of Polymers in Which Entanglements Greatly Outnumber Cross-Links. *Science* **2021**, *374* (6564), 212–216. https://doi.org/10.1126/science.abg6320.

(4) Liu, Y.; Ma, Y.; Zhao, Y.; Sun, X.; Gándara, F.; Furukawa, H.; Liu, Z.; Zhu, H.; Zhu, C.; Suenaga, K.; Oleynikov, P.; Alshammari, A. S.; Zhang, X.; Terasaki, O.; Yaghi, O. M. Weaving of Organic Threads into a Crystalline Covalent Organic Framework. *Science* **2016**, *351* (6271), 365–369. https://doi.org/10.1126/science.aad4011.

(5) Nosiglia, M. A.; Colley, N. D.; Danielson, M. K.; Palmquist, M. S.; Delawder, A. O.; Tran, S. L.; Harlan, G. H.; Barnes, J. C. Metalation/Demetalation as a Postgelation Strategy To Tune the Mechanical Properties of Catenane-Crosslinked Gels. *J. Am. Chem. Soc.* **2022**, *144* (22), 9990–9996. https://doi.org/10.1021/jacs.2c03166.

(6) Fielden, S. D. P.; Leigh, D. A.; Woltering, S. L. Molecular Knots. *Angew. Chem. Int. Ed.* **2017**, *56* (37), 11166–11194. https://doi.org/10.1002/anie.201702531.

(7) Guo, Q.-H.; Jiao, Y.; Feng, Y.; Stoddart, J. F. The Rise and Promise of Molecular Nanotopology. *CCS Chem.* **2021**, *3* (7), 1542–1572. https://doi.org/10.31635/ccschem.021.202100975.

(8) Prakasam, T.; Devaraj, A.; Saha, R.; Lusi, M.; Brandel, J.; Esteban-Gómez, D.; Platas-Iglesias, C.; Olson, M. A.; Mukherjee, P. S.; Trabolsi, A. Metal–Organic Self-Assembled Trefoil Knots

for C—Br Bond Activation. *ACS Catal.* **2019**, *9* (3), 1907–1914. https://doi.org/10.1021/acscatal.8b04650.
(9) Garci, A.; Weber, J. A.; Young, R. M.; Kazem-Rostami, M.; Ovalle, M.; Beldjoudi, Y.; Atilgan, A.; Bae, Y. J.; Liu, W.; Jones, L. O.; Stern, C. L.; Schatz, G. C.; Farha, O. K.; Wasielewski, M. R.; Fraser Stoddart, J. Mechanically Interlocked Pyrene-Based Photocatalysts. *Nat. Catal.* **2022**, *5* (6), 524–533. https://doi.org/10.1038/s41929-022-00799-y.
(10) David, A. H. G.; Stoddart, J. F. Chiroptical Properties of Mechanically Interlocked Molecules. *Isr. J. Chem.* **2021**, *61* (9–10), 608–621. https://doi.org/10.1002/ijch.202100066.
(11) August, D. P.; Borsley, S.; Cockroft, S. L.; della Sala, F.; Leigh, D. A.; Webb, S. J. Transmembrane Ion Channels Formed by a Star of David [2]Catenane and a Molecular Pentafoil Knot. *J. Am. Chem. Soc.* **2020**, *142* (44), 18859–18865. https://doi.org/10.1021/jacs.0c07977.
(12) Katsonis, N.; Lancia, F.; Leigh, D. A.; Pirvu, L.; Ryabchun, A.; Schaufelberger, F. Knotting a Molecular Strand Can Invert Macroscopic Effects of Chirality. *Nat. Chem.* **2020**, *12* (10), 939–944. https://doi.org/10.1038/s41557-020-0517-1.
(13) Danon, J. J.; Krüger, A.; Leigh, D. A.; Lemonnier, J.-F.; Stephens, A. J.; Vitorica-Yrezabal, I. J.; Woltering, S. L. Braiding a Molecular Knot with Eight Crossings. *Science* **2017**, *355* (6321), 159–162. https://doi.org/10.1126/science.aal1619.
(14) Ashbridge, Z.; Kreidt, E.; Pirvu, L.; Schaufelberger, F.; Stenlid, J. H.; Abild-Pedersen, F.; Leigh, D. A. Vernier Template Synthesis of Molecular Knots. *Science* **2022**, *375* (6584), 1035–1041. https://doi.org/10.1126/science.abm9247.
(15) Zhang, L.; Stephens, A. J.; Nussbaumer, A. L.; Lemonnier, J.-F.; Jurček, P.; Vitorica-Yrezabal, I. J.; Leigh, D. A. Stereoselective Synthesis of a Composite Knot with Nine Crossings. *Nat. Chem.* **2018**, *10* (11), 1083–1088. https://doi.org/10.1038/s41557-018-0124-6.
(16) Leigh, D. A.; Danon, J. J.; Fielden, S. D. P.; Lemonnier, J.-F.; Whitehead, G. F. S.; Woltering, S. L. A Molecular Endless (74) Knot. *Nat. Chem.* **2021**, *13* (2), 117–122. https://doi.org/10.1038/s41557-020-00594-x.
(17) Castle, T.; Evans, M. E.; Hyde, S. T. Ravels: Knot-Free but Not Free. Novel Entanglements of Graphs in 3-Space. *New J. Chem.* **2008**, *32* (9), 1484–1492. https://doi.org/10.1039/B719665B.
(18) Li, F.; Clegg, J. K.; Lindoy, L. F.; Macquart, R. B.; Meehan, G. V. Metallosupramolecular Self-Assembly of a Universal 3-Ravel. *Nat. Commun.* **2011**, *2* (1), 205. https://doi.org/10.1038/ncomms1208.
(19) Domoto, Y.; Fujita, M. Self-Assembly of Nanostructures with High Complexity Based on Metal⋯unsaturated-Bond Coordination. *Coord. Chem. Rev.* **2022**, *466*, 214605. https://doi.org/10.1016/j.ccr.2022.214605.
(20) Tamura, Y.; Takezawa, H.; Fujita, M. A Double-Walled Knotted Cage for Guest-Adaptive Molecular Recognition. *J. Am. Chem. Soc.* **2020**, *142* (12), 5504–5508. https://doi.org/10.1021/jacs.0c00459.
(21) Engelhard, D. M.; Freye, S.; Grohe, K.; John, M.; Clever, G. H. NMR-Based Structure Determination of an Intertwined Coordination Cage Resembling a Double Trefoil Knot. *Angew. Chem. Int. Ed.* **2012**, *51* (19), 4747–4750. https://doi.org/10.1002/anie.201200611.

(22) Bäuerle, P.; Ammann, M.; Wilde, M.; Götz, G.; Mena-Osteritz, E.; Rang, A.; Schalley, C. A. Oligothiophene-Based Catenanes: Synthesis and Electronic Properties of a Novel Conjugated Topological Structure. *Angew. Chem. Int. Ed.* **2007**, *46* (3), 363–368. https://doi.org/10.1002/anie.200602652.
(23) Götz, G.; Zhu, X.; Mishra, A.; Segura, J.-L.; Mena-Osteritz, E.; Bäuerle, P. π-Conjugated [2]Catenanes Based on Oligothiophenes and Phenanthrolines: Efficient Synthesis and Electronic Properties. *Chem. – Eur. J.* **2015**, *21* (19), 7193–7210. https://doi.org/10.1002/chem.201406039.
(24) Fan, Y.-Y.; Chen, D.; Huang, Z.-A.; Zhu, J.; Tung, C.-H.; Wu, L.-Z.; Cong, H. An Isolable Catenane Consisting of Two Möbius Conjugated Nanohoops. *Nat. Commun.* **2018**, *9* (1), 3037. https://doi.org/10.1038/s41467-018-05498-6.
(25) Bu, A.; Zhao, Y.; Xiao, H.; Tung, C.-H.; Wu, L.-Z.; Cong, H. A Conjugated Covalent Template Strategy for All-Benzene Catenane Synthesis. *Angew. Chem. Int. Ed. n/a* (n/a), e202209449. https://doi.org/10.1002/anie.202209449.
(26) Segawa, Y.; Kuwayama, M.; Hijikata, Y.; Fushimi, M.; Nishihara, T.; Pirillo, J.; Shirasaki, J.; Kubota, N.; Itami, K. Topological Molecular Nanocarbons: All-Benzene Catenane and Trefoil Knot. *Science* **2019**, *365* (6450), 272–276. https://doi.org/10.1126/science.aav5021.
(27) Segawa, Y.; Kuwayama, M.; Itami, K. Synthesis and Structure of [9]Cycloparaphenylene Catenane: An All-Benzene Catenane Consisting of Small Rings. *Org. Lett.* **2020**, *22* (3), 1067–1070. https://doi.org/10.1021/acs.orglett.9b04599.
(28) May, J.; Raden, J. V.; Maust, R.; Zakharov, L.; Jasti, R. Active Template Strategy for the Preparation of Interlocked Nanocarbons. **2022**. https://doi.org/10.26434/chemrxiv-2022-qh5f3.
(29) Schaufelberger, F.; Timmer, B. J. J.; Ramström, O. Principles of Dynamic Covalent Chemistry. In *Dynamic Covalent Chemistry*; John Wiley & Sons, Ltd, 2017; pp 1–30. https://doi.org/10.1002/9781119075738.ch1.
(30) Wang, Q.; Yu, C.; Long, H.; Du, Y.; Jin, Y.; Zhang, W. Solution-Phase Dynamic Assembly of Permanently Interlocked Aryleneethynylene Cages through Alkyne Metathesis. *Angew. Chem. Int. Ed.* **2015**, *54* (26), 7550–7554. https://doi.org/10.1002/anie.201501679.
(31) Rosenthal, U.; Ohff, A.; Baumann, W.; Tillack, A.; Görls, H.; Burlakov, V. V.; Shur, Vladimir. B. Struktur, Eigenschaften und NMR-spektroskopische Charakterisierung von Cp2Zr(Pyridin)(Me3SiC□CSiMe3). *Z. Für Anorg. Allg. Chem.* **1995**, *621* (1), 77–83. https://doi.org/10.1002/zaac.19956210114.
(32) Gessner, V. H.; Tannaci, J. F.; Miller, A. D.; Tilley, T. D. Assembly of Macrocycles by Zirconocene-Mediated, Reversible Carbon−Carbon Bond Formation. *Acc. Chem. Res.* **2011**, *44* (6), 435–446. https://doi.org/10.1021/ar100148g.
(33) Fujita, M.; Oguro, D.; Miyazawa, M.; Oka, H.; Yamaguchi, K.; Ogura, K. Self-Assembly of Ten Molecules into Nanometre-Sized Organic Host Frameworks. *Nature* **1995**, *378* (6556), 469–471. https://doi.org/10.1038/378469a0.
(34) Tozawa, T.; Jones, J. T. A.; Swamy, S. I.; Jiang, S.; Adams, D. J.; Shakespeare, S.; Clowes, R.; Bradshaw, D.; Hasell, T.; Chong, S. Y.; Tang, C.; Thompson, S.; Parker, J.; Trewin, A.; Bacsa, J.; Slawin, A. M. Z.; Steiner, A.; Cooper, A. I. Porous Organic Cages. *Nat. Mater.* **2009**, *8* (12), 973–978. https://doi.org/10.1038/nmat2545.

(35) Fujita, M.; Fujita, N.; Ogura, K.; Yamaguchi, K. Spontaneous Assembly of Ten Components into Two Interlocked, Identical Coordination Cages. *Nature* **1999**, *400* (6739), 52–55. https://doi.org/10.1038/21861.

(36) Yamauchi, Y.; Hanaoka, Y.; Yoshizawa, M.; Akita, M.; Ichikawa, T.; Yoshio, M.; Kato, T.; Fujita, M. M × n Stacks of Discrete Aromatic Stacks in Solution. *J. Am. Chem. Soc.* **2010**, *132* (28), 9555–9557. https://doi.org/10.1021/ja103180z.

Acknowledgements:

This work was funded by the National Science Foundation under Grant No. CHE-2103696. Work performed at the Molecular Foundry was supported by the Office of Science, Office of Basic Energy Sciences, US Department of Energy under contract no. DE-AC02-05CH11231. We thank Dr. Hasan Celik and UC Berkeley's NMR facility in the College of Chemistry (CoC-NMR) for spectroscopic assistance. Instruments in the CoC-NMR are supported in part by NIH S10OD024998. We thank Dr. Simon Teat (ALS, LBNL) for providing a preliminary crystallographic solution of **3-Zr** (via The Advanced Light Source, which is supported by the Director, Office of Science, Office of Basic Energy Sciences, U.S. Department of Energy under contract no. DE-AC02-05CH11231) that enabled early confirmation of its structure. We thank Dr. Zoe Ashbridge for helpful discussions about topological nomenclature concerning compound **3**. We thank Rob Scharien for guidance and technical support in using his KnotPlot software to visualize the perplexanes in Figure 2.